P. J. Coelho
Assistant Professor

M. G. Carvalho
Professor,

Mechanical Engineering Department,
Instituto Superior Técnico
Technical University of Lisbon,
Av. Rovisco Pais,
1096 Lisboa Codex,
Portugal

# A Conservative Formulation of the Discrete Transfer Method

*The discrete transfer method, often employed to calculate radiative heat transfer in combustion chambers, is not conservative. The reason for this behavior is examined and a conservative formulation is proposed and evaluated. A simple treatment of isotropic scattering media is also presented. The original and the conservative formulation of the method are applied to two-dimensional and three-dimensional enclosures containing a participating medium. It is shown that the accuracy of the original and the conservative formulation is very similar, but the proposed formulation has the advantage of ensuring energy conservation.*

## Introduction

Radiative heat transfer plays an important role in many engineering problems, especially in aeronautics, astronautics, and mechanics, and it is the dominant heat transfer mechanism in many industrial combustion equipments, including boilers and furnaces. Hence, the accurate prediction of the heat transferred by radiation is a key issue in the design and operation of combustion chambers. In this case, the calculation of radiative heat transfer is part of a more complex problem which involves the numerical simulation of a turbulent reactive flow.

Although many radiation models have been developed for emitting, absorbing, and scattering media (e.g., Viskanta and Mengüç, 1987), generally based on the solution of the radiative heat transfer equation (RTE), most of them are not recommended for coupled fluid flow/heat transfer problems. Despite their recognized accuracy, some methods, such as the zonal (Hottel and Sarofim, 1967) and the Monte Carlo (Howell, 1968) methods, require long computing times and involve numerical algorithms very different from those employed in fluid flow calculations. Others, such as the flux method of Schuster-Schwarzchild and its generalization for two- and three-dimensional domains (Selçuk 1983), have low accuracy. The spherical harmonics method (e.g., Mengüç and Viskanta, 1985) is not accurate for low order approximations, except in optically thick media, and the increase of accuracy achievable using high order approximations is mathematically involved (Modest, 1993). Three of the most attractive methods, as far as accuracy and computational requirements are concerned, are the discrete transfer (Shah, 1979; Lockwood and Shah, 1981), the discrete ordinates (Carlson and Lathrop, 1968; Fiveland, 1984), and the finite volume method (Raithby and Chui, 1990; Chai et al., 1994). They are easily incorporated in reactive fluid flow codes and a comparative study of their performance for several benchmark problems has recently been published (Coelho et al., 1995).

Lockwood and Shah (1981) claim that the discrete transfer method (DTM) is economical, straightforwardly applicable to complex geometries, easy to apply, and able to return any desired degree of precision. These features justify its popularity and wide application in calculations in combustion chambers (e.g., Gosman et al., 1982; Boyd and Kent, 1986; Carvalho and Coelho, 1989), as well as its incorporation in commercial computational fluid dynamics codes, such as FLUENT and FLOW3D. However, since the method was proposed by Lockwood and Shah, only a few fundamental studies or extensions have been reported. Murthy and Choudhury (1992) applied the method to two-dimensional domains of arbitrary shape and Carvalho et al. (1993) studied two- and three-dimensional enclosures containing a scattering medium. Recently, Bressloff et al. (1995) proposed a new set of weighting coefficients for the radiation intensity along each ray tracing direction. The new weighting set is based on the discretization of the hemispherical solid angle using quasi-equal solid angles in an attempt to provide a more even distribution of ray directions and to mitigate the ray effect. More accurate quadrature formulae for the calculation of the incident heat flux have been developed by Cumber (1995). In the proposed formulae, the incident intensity is assumed to vary within each solid angle resultant from the discretization of the hemisphere, rather than being constant, as in the original method. Similarly, when integrating the RTE, the temperature is assumed to vary linearly in each control volume.

A major shortcoming of the DTM, which has not been addressed in the literature, is that, in general, the method is not conservative if the boundary temperature is prescribed, i.e., the numerical solution calculated by the DTM does not satisfy the principle of conservation of energy. This is in contrast with other competitive methods, namely the discrete ordinates and the finite volume method, which are conservative. The present work explains why, in general, the DTM is not conservative and proposes a simple correction to overcome this problem. In addition, it employs a treatment of isotropic scattering simpler and more accurate than that proposed by Lockwood and Shah (1981) and used in Carvalho et al. (1993).

A brief description of the method is given in the next section. Then, the conservation problem is addressed and two different modifications are proposed. These are evaluated by means of the application of the different formulations to benchmark problems. The results obtained are presented and discussed, and the paper ends with a summary of the main conclusions.

## The Discrete Transfer Method

**Original Formulation.** The main features of the DTM are described below in order to facilitate the discussion of the conservation problem. A complete description of the method is given by Lockwood and Shah (1981).

The DTM is based on the numerical solution of the RTE along specified directions. For a gray medium, as considered in this paper, the RTE may be written as follows (e.g., Modest, 1993):

$$\frac{dI}{ds} = -\beta I + \kappa I_b + \frac{\sigma_s}{4\pi}\int_0^{4\pi} I(\vec{s}')\phi(\vec{s}', \vec{s})d\Omega' \qquad (1)$$

The ratio $\phi(\vec{s}', \vec{s})/4\pi$ represents the probability that radiation propagating in the direction $\vec{s}'$ and confined within the solid

Contributed by the Heat Transfer Division for publication in the Journal of Heat Transfer. Manuscript received by the Heat Transfer Division October 2, 1995; revision received September 25, 1996; Keywords: Conjugate Heat Transfer, Numerical Methods, Radiation. Associate Technical Editor: M. Modest.

angle $d\Omega'$ is scattered through the angle $(\vec{s}', \vec{s})$ into the direction $\vec{s}$ confined within the solid angle $d\Omega$. The absorption, scattering, and extinction coefficients are related to the single scattering albedo as follows:

$$\omega = \sigma_s/(\kappa + \sigma_s) = \sigma_s/\beta \qquad (2)$$

Equation (1) is a statement of the principle of conservation of energy applied to a pencil of radiation traveling along direction $\vec{s}$.

In the DTM the physical domain is divided into control volumes (CV). The temperature and the radiative properties of the medium are taken as constant in each one of them. For all the CV adjacent to the boundary, the central points of the faces of the CV coincident to the boundary are determined. Let $P_j$ be one of such points. The hemisphere centered at $P_j$ is discretized into a prescribed number of solid angles. Each solid angle defines a direction along which the RTE is solved.

Hence, given a point $P_j$ at the center of a cell face on the boundary, a radiation beam is fired from $P_j$ for each one of the directions specified above (Fig. 1). The path of a radiation beam is followed until it hits another boundary. Let $Q_i$ be the impingement point. Although, in general, $Q_i$ is not the central point of a boundary cell, it is assumed that the radiation intensity at $Q_i$ and at the central point of the boundary cell which contains $Q_i$ are equal. Then, starting from $Q_i$, the path of the beam is followed back to the origin (point $P_j$) and the RTE is integrated analytically along this path. Henceforth, the radiation beam traveling from $P_j$ to $Q_i$ will be referred to as a radiosity ray, and the radiation beam traveling back from $Q_i$ to $P_j$ will be referred to as an irradiation ray. The starting point of a radiosity ray and the ending point of an irradiation ray are always the center of a cell face on the boundary. On the contrary, the ending point of a radiosity ray and the starting point of an irradiation ray do not usually coincide with the center of a boundary cell face.

The integration of the RTE yields (Lockwood and Shah, 1981):

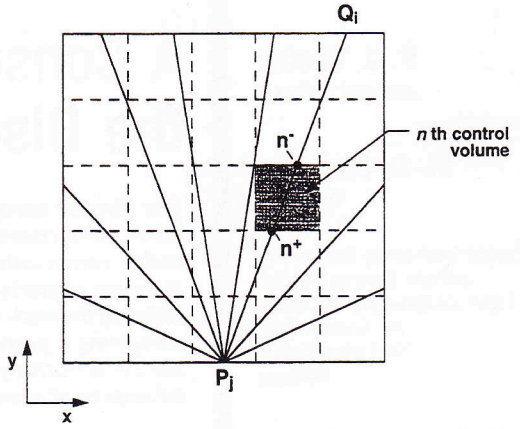


**Fig. 1 Projection onto the x-y plane of the radiation beams resultant from the discretization of the hemisphere centered at the boundary point $P_j$**

$$I_{n^+,i\to j} = I_{n^-,i\to j}e^{-\beta\delta s} + \Big[(1-\omega)I_b + (\omega/4\pi)\int_0^{4\pi} I(\vec{s}')\phi(\vec{s}', \vec{s})d\Omega'\Big](1 - e^{-\beta\delta s}) \qquad (3)$$

where the subscript $i \to j$ identifies the direction of the irradiation ray traveling from $Q_i$ to $P_j$, and the subscripts $n^-$ and $n^+$ denote the points where that ray enters and leaves the $n$th CV, respectively (Fig. 1). In the CV where the irradiation ray originates, $n^-$ coincides with $Q_i$; in the control volume where the irradiation ray hits the boundary, $n^+$ coincides with $P_j$.

The incident radiative heat flux at point $P_j$, i.e., the irradiation, is calculated by adding the contributions due to all the irradiation rays that reach point $P_j$ (one for each solid angle

## Nomenclature

$A$ = Area
$C$ = Correction factor
$D_{j,i}$ = Integral of cos $\theta_{j,i}$ over a solid angle element associated with the direction $j \to i$
$E$ = Absolute error
$E_1, E_2, E_3$ = Unsteady, conductive and radiative terms of the energy equation integrated in space and time
$G$ = Incident radiation
$H$ = Irradiation onto a surface
$I$ = Radiation intensity
$I_{k,i\to j}$ = Radiation intensity at point $k$ of an irradiation ray traveling in direction $i \to j$
$J$ = Radiosity
$k$ = Thermal conductivity
$\vec{n}$ = Unit surface normal
$N$ = Conduction-to-radiation parameter
$NI$ = Number of control volumes along $x$ direction
$NJ$ = Number of control volumes along $y$ direction
$N_\theta$ = Number of $\theta$ angles per octant
$N_\varphi$ = Number of $\varphi$ angles per octant
$q$ = Radiative heat flux
$Q$ = Dimensionless heat flux
$\bar{Q}$ = Volumetric heat source
$s$ = Geometric path length
$\vec{s}$ = Unit vector into a given direction
$S$ = Radiative source term of the energy conservation equation
$t$ = Time
$T$ = Temperature
$\alpha$ = Thermal diffusivity
$\beta$ = Extinction coefficient
$\delta s$ = Optical length within a control volume
$\Delta t^*$ = Time step
$\Delta V$ = Volume
$\Delta\theta$ = Discrete polar angle
$\Delta\varphi$ = Discrete azimuthal angle
$\Delta\Omega_{j,i}$ = Discrete solid angle associated with the direction $j \to i$
$\epsilon$ = Emissivity
$\eta$ = Relative error
$\theta$ = Polar angle; dimensionless temperature
$\theta_{j,i}$ = Angle between the surface normal at $P_j$ and the direction $j \to i$
$\kappa$ = Absorption coefficient
$\sigma$ = Stefan-Boltzmann constant
$\sigma_s$ = Scattering coefficient
$\tau$ = Optical coordinate
$\phi$ = Scattering phase function
$\varphi$ = Azimuthal angle
$\psi$ = Dimensionless radiation intensity
$\omega$ = Single scattering albedo
$\Omega$ = Solid angle

### Subscripts

avg = Averaged value over a control volume
$b$ = Blackbody value
$g$ = Gas
$j \to i$ = Direction from point $P_j$ to point $Q_i$
$n$ = Control volume
$n^-, n^+$ = Entry ($n^-$) into or exit ($n^+$) from a control volume
$o$ = Reference value
$P$ = Point P
$x, y$ = Cartesian coordinates
$w$ = Wall

### Superscripts

* = Dimensionless quantity
− = Mean value

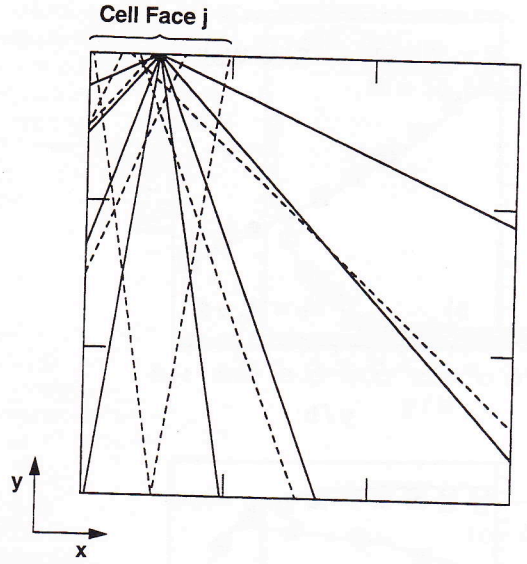


Fig. 2 Projection onto the $x$-$y$ plane of all the irradiation rays that arrive (solid lines) or start (dashed lines) at the boundary cell face centered at $P_j$, for $NI = NJ = 3$ and $N_\theta = N_\varphi = 2$

resultant from the discretization of the hemisphere centered at $P_j$):

$$H_j = \int_0^{2\pi} I(\vec{s})\vec{n}.\vec{s}\,d\Omega \approx \sum_i I_{j,i\to j} D_{j,i}\,. \tag{4}$$

$I_{j,i\to j}$ is the radiation intensity at point $P_j$ of the irradiation ray traveling from $Q_i$ to $P_j$. It is important to point out that only the radiation intensity of irradiation rays is involved in DTM calculations. $D_{j,i}$ is the integral of the cosine of the angle $\theta_{j,i}$ between the surface normal at $P_j$ and the direction $j \to i$ over a solid angle element $\Delta\Omega_{j,i}$:

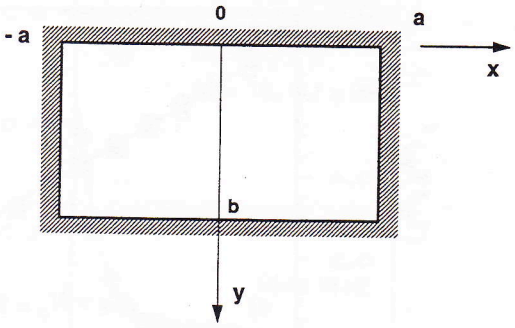


Fig. 3 Geometry of test case 1

$$D_{j,i} = \int_{\Delta\Omega_{j,i}} \cos\theta_{j,i}\,d\Omega$$
$$= \cos\theta_{j,i}\,\sin\theta_{j,i}\,\sin(\Delta\theta_{j,i})\Delta\varphi_{j,i}\,. \tag{5}$$

Since the solid angles ($\Delta\Omega_{j,i}$) are defined from the discretization of a hemisphere centered at $P_j$, the following identity holds: $\sum_i D_{j,i} = \pi$.

The solution of the RTE requires the specification of the boundary conditions. If the wall temperature is prescribed, the boundary condition for a gray diffuse boundary surface may be written as follows:

$$J_j = \epsilon_w \sigma T_w^4 + (1 - \epsilon_w) H_j. \tag{6}$$

The calculation procedure is iterative, unless $\epsilon_w = 1$, because the radiation intensities of the irradiation rays at the points $Q_i$ are not known a priori. Other boundary conditions may be treated as described by Lockwood and Shah (1981).

The radiation source (or sink) for each CV, which appears in the energy conservation equation, may be defined as

Table 1 Ratio between the heat rate received and the heat rate leaving the boundary of the enclosure of test case 1 calculated using DTM-0, mean absolute errors of the normalized incident heat flux on the boundary, and normalized emissive power at $x = 0$

| a/b | NI x NJ | $N_\theta$ x $N_\varphi$ | $\frac{\sum A_j H_j}{\sum A_j J_j}$ | $\bar{E}(q/\sigma T_w^4) \times 10^2$ | | | $\bar{E}(T_g^4/T_w^4) \times 10^2$ | | |
|---|---|---|---|---|---|---|---|---|---|
| | | | | DTM-0 | DTM-1 | DTM-2 | DTM-0 | DTM-1 | DTM-2 |
| 0.2 | 10 x 20 | 2 x 2 | 0.8750 | 1.38 | 1.41 | — | 3.04 | 3.22 | — |
| | 10 x 20 | 5 x 5 | 0.9984 | 0.38 | 0.38 | 0.41 | 0.85 | 0.85 | 0.80 |
| | 20 x 40 | 2 x 2 | 1.0000 | 1.30 | 1.30 | 1.36 | 2.78 | 2.78 | 2.88 |
| | 20 x 40 | 5 x 5 | 1.0426 | 0.44 | 0.43 | 0.46 | 0.74 | 0.72 | 0.77 |
| | 40 x80 | 2 x 2 | 0.9063 | 1.39 | 1.37 | 1.53 | 2.84 | 2.81 | 3.26 |
| | 40 x80 | 5 x 5 | 1.0267 | 0.43 | 0.43 | 0.52 | 0.74 | 0.72 | 1.05 |
| | 40 x80 | 10 x 10 | 1.0262 | 0.15 | 0.14 | 0.14 | 0.59 | 0.46 | 0.51 |
| 5 | 20 x 10 | 2 x 2 | 1.0125 | 3.09 | 2.71 | 2.89 | 0.81 | 0.83 | 2.02 |
| | 20 x 10 | 5 x 5 | 1.0002 | 1.12 | 1.11 | 1.06 | 0.23 | 0.23 | 0.52 |
| | 40 x 20 | 2 x 2 | 1.0000 | 3.19 | 3.19 | 3.01 | 0.81 | 0.81 | 1.75 |
| | 40 x 20 | 5 x 5 | 0.9957 | 1.35 | 1.19 | 1.30 | 0.25 | 0.32 | 0.67 |
| | 80 x 40 | 2 x 2 | 1. 0094 | 3.06 | 2.88 | 3.15 | 0.81 | 0.81 | 1.67 |
| | 80 x 40 | 5 x 5 | 0.9973 | 1.25 | 1.18 | 1.30 | 0.26 | 0.29 | 0.67 |
| | 80 x 40 | 10 x 10 | 0.9974 | 0.94 | 0.84 | 0.77 | 0.17 | 0.19 | 0.19 |

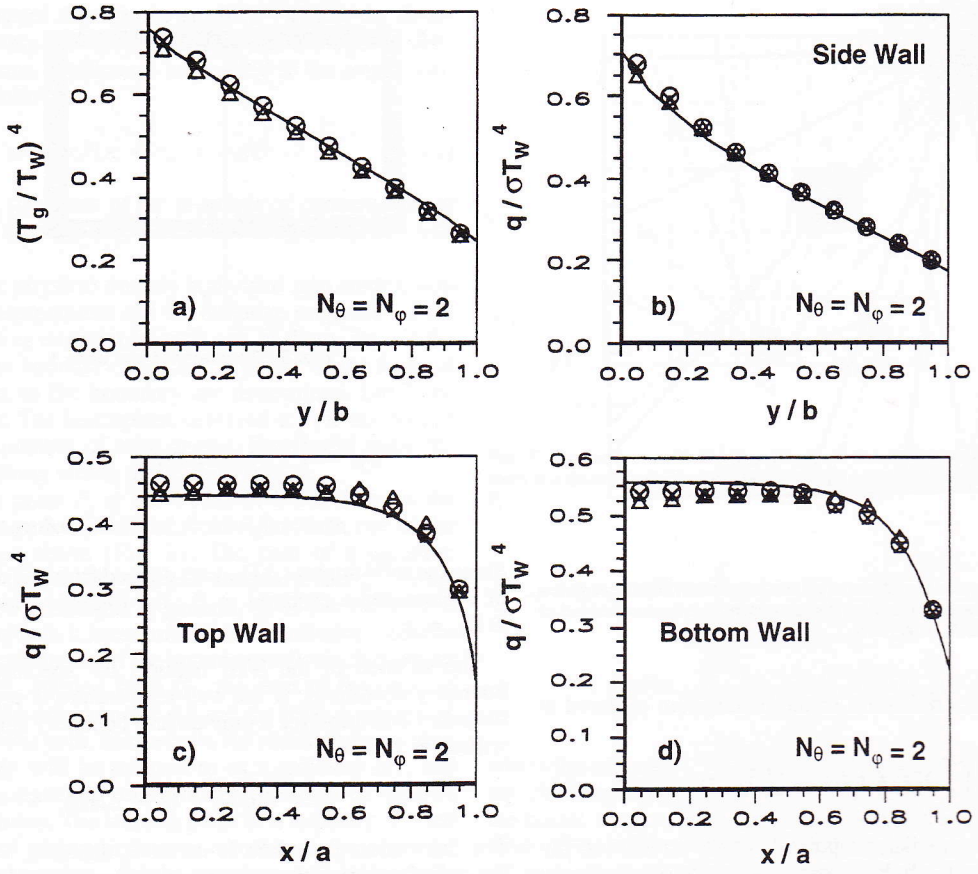


**Fig. 4 Predictions for test case 1 with $a/b = 5$ and $N_\theta = N_\varphi = 2$ (solid line: Crosbie and Schrenker; O-DTM-0, X-DTM-1; Δ-DTM-2): (*a*) normalized emissive power at $x = 0$; (*b*) normalized incident heat flux on side wall; (*c*) normalized incident heat flux on top wall; and (*d*) normalized incident heat flux on bottom wall.**

$$S = \int_{CS} \vec{q}.\vec{n}dA = \int_{CS}\int_0^{4\pi} I(\vec{s})\vec{n}.\vec{s}d\Omega dA \qquad (7)$$

where $\vec{q}$ is the radiative heat flux vector and the integration is carried out over the surface area, CS, of the CV. However, the DTM does not perform a discretization of the RTE over a CV. Therefore, the source term $S$ is not evaluated from the discretization of Eq. (7). Instead, the source term for a CV is obtained from the sum of the contributions of all the irradiation rays which cross that CV. It is assumed that the contribution of each irradiation ray is proportional to the change of the radiation intensity leaving and entering that CV. This yields the following equation:

$$S_n = \sum_j \sum_i (I_{n^+,i\to j} - I_{n^-,i\to j}) D_{j,i} A_j \qquad (8)$$

In this equation, index $j$ runs over all the boundary cell faces and index $i$ extends over all the irradiation rays hitting cell face $j$. If an irradiation ray traveling from $Q_i$ to $P_j$ does not cross the $n$th CV then $I_{n^+,i\to j} = I_{n^-,i\to j} = 0$.

**Consideration of Scattering.** The calculation of radiative heat transfer in scattering media requires the computation of the integral which appears in the in-scattering term (Eq. 3). Lockwood and Shah (1981) have approximated this integral as

$$\int_0^{4\pi} I(\vec{s}')\phi(\vec{s}', \vec{s})d\Omega' \approx \sum (I(\vec{s}'))_{avg}\phi(\vec{s}', \vec{s})\Delta\Omega' \qquad (9)$$

where the averaged intensity is taken as the arithmetic mean of the radiation intensity at the inlet and outlet of the CV. The summation extends over all the irradiation rays that cross the CV. This approximation was successfully used by Carvalho et al. (1993) for isotropic scattering media, and we are not aware of any attempt to apply it for anisotropic scattering media.

In the case of isotropic scattering, however, the approximation used in Eq. (9) can be avoided. In fact, in this case the scattering phase function is equal to one. Therefore, the integral in the in-scattering term is equal to the incident radiation

$$\int_0^{4\pi} I(\vec{s}')\phi(\vec{s}', \vec{s})d\Omega' = G. \qquad (10)$$

If the equation for the conservation of radiative energy (e.g., Modest, 1993)

$$\nabla . q = \kappa(4\sigma T^4 - G) \qquad (11)$$

is integrated over the CV, the left hand side yields the radiation source (or sink) of the energy conservation equation, $S$. Therefore, Eq. (11) can be used to compute $G$ as

$$G = 4\sigma T^4 - \frac{S}{\kappa\Delta V}. \qquad (12)$$

In this way, the in-scattering term is easily obtained without the approximation embodied in Eq. (9). In the case of pure scattering ($\kappa = 0$), Eq. (12) is not applicable. However, the case of pure scattering is mathematically equivalent to an absorbing-emitting medium in radiative equilibrium (Modest, 1993). Therefore, in such a case the incident radiation is given by $G = 4\sigma T^4$.

**Conservative and Non-Conservative Formulations.** A desirable feature of any solution method for the RTE is that the numerical solution satisfies conservation of energy. However, in general, the numerical solution obtained using the DTM does

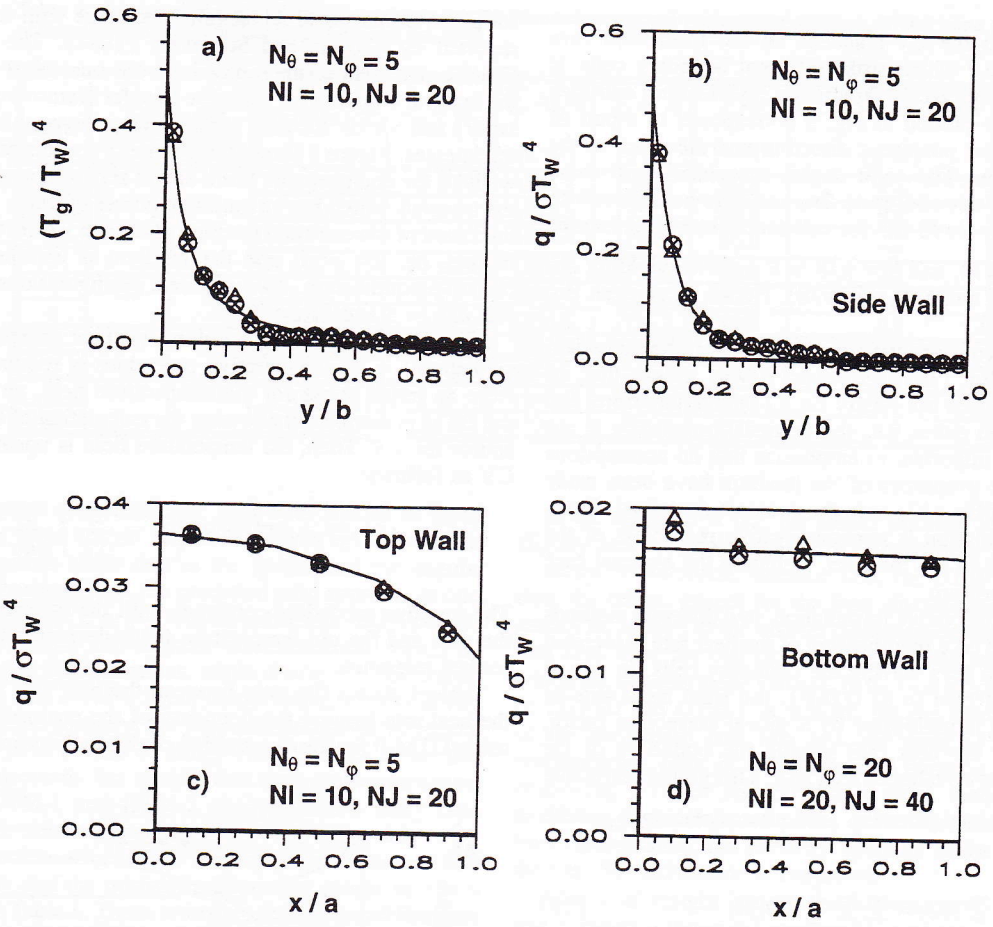


**Fig. 5** Predictions for test case 1 with $b/a = 5$ (solid line: Crosbie and Schrenker; O-DTM-0; X-DTM-1; Δ-DTM-2): (*a*) normalized emissive power at $x = 0$; (*b*) normalized incident heat flux on side wall; (*c*) normalized incident heat flux on top wall; and (*d*) normalized incident heat flux on bottom wall.

not satisfy this principle. The reason why this happens is examined below and alternative conservation formulations are proposed.

If thermal radiation is the only mechanism of heat transfer present, the principle of conservation of energy applied to an enclosure states that the net heat rate leaving the enclosure through its boundary is equal to the difference between the radiative energy generated (emitted) and destroyed (absorbed) within the enclosure per unit time. Mathematically, this means that

$$\sum_j A_j(H_j - J_j) = \sum_n S_n \tag{13}$$

where the summation on the left hand side runs over all the cell faces on the boundary and that on the right hand side extends over all the control volumes. This equation is also valid for a scattering medium since scattering only redirects radiation beams and does not change the energy balance.

From Eq. (8), the radiative heat source in the enclosure may be expressed, using the commutative law of addition, as

$$\sum_n S_n = \sum_j \sum_i [\sum_n (I_n^+{}_{,i\to j} - I_n^-{}_{,i\to j})] D_{j,i} A_j. \tag{14}$$

The term in the square brackets represents the change of the radiation intensity of an irradiation ray along its path from $Q_i$ to $P_j$. Therefore, Eq. (14) may be written as

$$\sum_n S_n = \sum_j \sum_i (I_{j,i\to j} - I_{i,i\to j}) D_{j,i} A_j. \tag{15}$$

Inserting Eqs. (4) and (15) into Eq. (13) and simplifying, results in

$$\sum_j A_j J_j = \sum_j \sum_i I_{i,i\to j} D_{j,i} A_j. \tag{16}$$

Interchanging indices $i$ and $j$ on the right hand side of this equation, and applying the commutative law of addition, yields the following:

$$\sum_j A_j J_j = \sum_j \sum_i I_{j,j\to i} D_{i,j} A_i. \tag{17}$$

In this equation, index $j$ runs over all the cell faces on the boundary, and index $i$ extends over all the irradiation rays traveling in direction $j \to i$.

In the DTM, the irradiation rays that start at cell face $j$ and travel in direction $j \to i$ are not associated with the discretization of a hemisphere centered at a point on the boundary cell face $j$. Hence, the number of these irradiation rays may change from cell to cell and, in general, for a given cell $j$, it will be $\sum_i D_{i,j} \neq \pi$ (in contrast to $\sum_i D_{j,i} = \pi$), as illustrated below using a simple example. Therefore, setting $I_{j,j\to i} = J_j/\pi$ for diffusely emitting-reflecting boundaries, Eq. (17) is not generally satisfied, even if the areas are all equal.

As an example, consider a two-dimensional square enclosure discretized using a uniform grid with $3 \times 3$ control volumes and four solid angles per octant ($N_\theta = N_\varphi = 2$). Although these spatial and angular discretizations may be too coarse if an accurate solution is sought, they are adequate for the present purpose. Figure 2 shows the projection onto the $x$-$y$ plane of all the irradiation rays that hit cell face $j$. The solid angles associated with these rays have resulted from the discretization of a hemisphere and, therefore, $\sum_i D_{j,i} = \pi$. Figure 2 also shows

the projection onto the $x$-$y$ plane of all the irradiation rays starting at cell face $j$ which strike different boundary cells. It can be seen that there are 14 irradiation rays leaving cell face $j$. Each dashed line plotted in Fig. 2 corresponds to a pair of rays, one fired in the positive $z$ direction and the other in the negative $z$ direction. The solid angles associated with these irradiation rays do not add up to $2\pi$, and it is not difficult to verify that $\sum_i D_{i,j} = 7\pi/8$ for the cell face $j$ in Fig. 2 (notice that $\Delta\theta = \Delta\varphi = \pi/4$, and $\theta = \pi/8$ or $\theta = 3\pi/8$, yielding $D_{i,j}$ = constant = $\pi/16$ and $\sum_i D_{i,j} = 7\pi/8$). Hence, in general, Eq. (17) is not satisfied.

A solution method is conservative if and only if the numerical solution satisfies Eq. (13). However, it was shown that, in general, the DTM does not satisfy Eq. (17) and, therefore, Eq. (13) is not satisfied either, i.e., the original formulation is not conservative. It is important to emphasize that no assumptions about the radiative properties of the medium have been made in the derivation of Eq. (17) or in the example described above. The original formulation is nonconservative regardless of the radiative properties of the medium, including the especial case of a transparent medium.

To achieve a conservative formulation, two different methods are proposed based on a modification of the heat rate associated with the irradiation rays leaving the boundary cells. In one of them, hereafter referred to as DTM-1, the right hand side of Eqs. (14) to (17) is multiplied by a global correction factor, $C$, to ensure that the heat rate leaving the boundary of the enclosure is correctly evaluated as $\sum_j A_j J_j$. This global correction factor may be obtained from Eq. (17) after replacing $I_{j,j\to i}$ with $J_j/\pi$,

$$\sum_j A_j J_j = \sum_j \sum_i \frac{J_j}{\pi} C D_{i,j} A_i \tag{18}$$

yielding

$$C = \frac{\sum_j A_j J_j}{\sum_j J_j (\sum_i D_{i,j} A_i/\pi)}. \tag{19}$$

This is mathematically equivalent to set $I_{i,i\to j} = CJ_i/\pi$ when applying Eq. (3) to the irradiation ray starting at cell face $i$.

In the other modification, which will be referred to as DTM-2, a local correction factor, $C_j$, is applied to each boundary cell, such that

$$A_j J_j = \sum_i \frac{J_j}{\pi} C_j D_{i,j} A_i \tag{20}$$

yielding

$$C_j = \frac{A_j}{\sum_i D_{i,j} A_i/\pi}. \tag{21}$$

The DTM-2 can be applied only if there is at least one irradiation ray leaving every boundary cell. Otherwise, the denominator in Eq. (21) will be zero. However, this situation is likely to occur only if coarse angular discretizations are used.

Both DTM-1 and DTM-2 are conservative, i.e., the numerical solution satisfies Eq. (13); they are evaluated below and compared with the original method (DTM-0).

## Evaluation of the Conservative Formulations

**Test Case 1—Two-Dimensional Rectangular Enclosure With an Emitting-Absorbing Medium.** Evaluation of the conservative formulations for an emitting-absorbing medium was undertaken by comparison of the predictions of the DTM for a two-dimensional rectangular enclosure with the solutions reported by Crosbie and Schrenker (1984). The method of Crosbie and Schrenker is based on the numerical solution of the integral equation for radiative transfer (removing the singularity) and yields accurate results except at very large optical thicknesses. Figure 3 shows the geometry for this problem. The walls of the enclosure are black and at zero temperature, except the top wall which has an emissive power of unity. The optical thickness of the enclosed medium along the $y$ direction is equal to one, i.e., $\beta b = 1$, and the medium is assumed to be in radiative equilibrium. Two different configurations were studied: $a/b = 5$ and $b/a = 5$.

Since, in this problem, a volumetric heat source, $\dot{Q}$, is prescribed ($\dot{Q} = 0$), an iterative procedure is required. Starting from an initial guess for the temperature field, an iteration of the DTM is carried out allowing the calculation of the radiative source term $S$. Then, the temperature field is updated for each CV as follows:

$$(T^4)^{\text{new}} = (T^4)^{\text{old}} + \left(\dot{Q} - \frac{S}{\Delta V}\right)\frac{1}{4\kappa\sigma}. \tag{22}$$

The iterative procedure continues until the difference between the new and the old temperature fields decreases below a prescribed tolerance.

Table 1 shows the ratio between the heat rate received and the heat rate leaving the boundary of the enclosure calculated using DTM-0 for the two studied configurations and for several

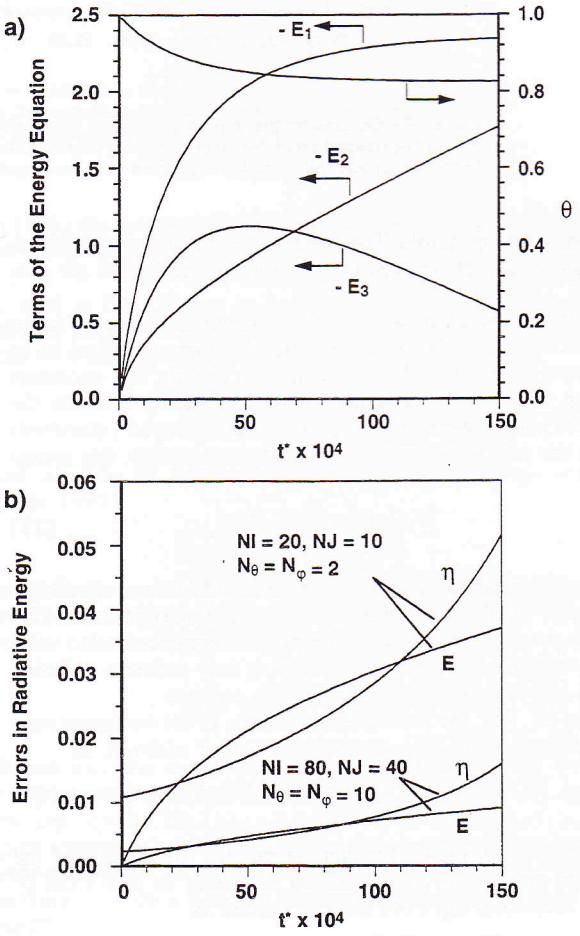


**Fig. 6 Transient combined conduction-radiation problem in a two-dimensional enclosure: (*a*) terms of the energy conservation equation integrated in time and over the whole enclosure (Eq. 28), and dimensionless temperature at the center of the enclosure; (*b*) absolute and relative errors of the radiative energy $E_3$.**

Table 2 Terms of the global energy balance for the three-dimensional rectangular furnace of test case 3 calculated using the original formulation of the DTM

| Run | $\kappa$ ($m^{-1}$) | $\sigma_s$ ($m^{-1}$) | NIxNJxNK | $N_\theta \times N_\varphi$ | $\sum_j A_j H_j$ (kW) | $\sum_j A_j J_j$ (kW) | $\sum_n S_n$ (kW) | $\sum_j A_j (H_j - J_j) - \sum_n S_n$ (kW) |
|---|---|---|---|---|---|---|---|---|
| 1 | 0.25 | 0 | 9 x 9 x 15 | 2 x 2 | 1844.3 | 1760.7 | 80.0 | 3.6 |
| 2 | | | 9 x 9 x 15 | 5 x 5 | 1840.5 | 1759.7 | 80.0 | 0.8 |
| 3 | | | 27 x 27 x 45 | 5 x 5 | 1839.4 | 1759.2 | 80.0 | 0.2 |
| 4 | | | 27 x 27 x 45 | 10 x 10 | 1838.6 | 1759.0 | 80.0 | 0.4 |
| 5 | 0.5 | 0 | 9 x 9 x 15 | 2 x 2 | 1840.4 | 1756.8 | 80.0 | 3.6 |
| 6 | | | 9 x 9 x 15 | 5 x5 | 1836.6 | 1755.7 | 80.0 | 0.9 |
| 7 | 1.0 | 0 | 9 x 9 x 15 | 2 x 2 | 1834.8 | 1751.0 | 80.0 | 3.8 |
| 8 | | | 9 x 9 x 15 | 5 x 5 | 1830.9 | 1750.0 | 80.0 | 0.9 |
| 9 | 0.15 | 0.35 | 9 x 9 x 15 | 2 x2 | 1840.4 | 1756.8 | 80.0 | 3.6 |
| 10 | | | 9 x 9 x 15 | 5 x 5 | 1836.6 | 1755.7 | 80.0 | 0.9 |

spatial and angular discretizations. This ratio should be equal to one because there are no radiative sources or sinks in the medium. The results show that as the spatial and the angular discretizations become finer, the predicted ratio approaches one, but not monotonically. If $a/b = 0.2$, an imbalance of 2.6 percent occurs for fine spatial and angular discretizations, which increases for coarser discretizations, while if $a/b = 5$, the imbalance is smaller. The DTM-0 is not conservative, except in two of the cases. On the contrary, the proposed conservative formulations always yield a ratio of unity. This does not mean that they are more accurate, but simply that they are conservative. Indeed, both DTM-1 and DTM-2 always yield a unity ratio regardless of the solution accuracy.

The mean absolute errors of the normalized incident heat flux on the boundary and the normalized emissive power at $x = 0$ are also listed in Table 1. These errors are defined as the absolute value of the difference between the numerical solution and the reference solution of Crosbie and Schrenker, averaged over all the cell faces on the boundary, for the incident heat fluxes, or over all the CV crossing the line $x = 0$, for the emissive power. The results show that the solution accuracy is only marginally influenced by the spatial grid refinement, regardless of the method employed. On the contrary, a finer angular discretization yields improved accuracy.

In the case $a/b = 0.2$, the results obtained using DTM-1 are slightly more accurate than those calculated by means of DTM-0, except for the coarser discretization. The DTM-2 is less accurate than the others, except for the finer discretization. Moreover, it cannot be applied to the coarser discretization because no irradiation rays leave the cell faces on the top and bottom boundaries which are adjacent to the vertices. In the case $a/b = 5$, the accuracy of DTM-0 and DTM-1 is similar, but the mean absolute error of the normalized heat flux is lower using DTM-1, while the corresponding error of the normalized emissive power is lower employing DTM-0. The DTM-2 is much worse regarding the prediction of the emissive power of the medium, except for the finer discretization, but performs similarly to the others as far as the heat flux calculation is concerned.

Additional insight into the predictions is provided in Figs. 4 and 5. Figure 4 shows the predicted results obtained for a rectangular slab with $a/b = 5$ using a grid with $20 \times 10$ CV and $N_\theta = N_\varphi = 2$; they closely follow the solution of Crosbie and Schrenker. As expected from the ratio $\Sigma_i A_i H_i / \Sigma_i A_i J_i = 1.0125$ and from the mean absolute errors (Table 3), the results computed using DTM-0 and DTM-1 are almost identical.

The columnar shaped geometry with $b/a = 5$ was studied using a grid with $10 \times 20$ CV and $N_\theta = N_\varphi = 5$. The predictions

Table 3 Mean relative errors of temperature and net heat fluxes for test case 3; the runs are characterized in Table 2

| Run | $\overline{\eta}(T) \times 10^2$ | | | $\overline{\eta}(q) \times 10^2$ | | |
|---|---|---|---|---|---|---|
| | DTM-0 | DTM-1 | DTM-2 | DTM-0 | DTM-1 | DTM-2 |
| 1 | 1.03 | 1.01 | 1.37 | 2.78 | 2.77 | 6.00 |
| 2 | 0.33 | 0.33 | 0.38 | 0.84 | 0.86 | 1.03 |
| 3 | 0.31 | 0.31 | 0.41 | 0.79 | 0.80 | 1.00 |
| 4 | 0.27 | 0.27 | 0.26 | 0.81 | 0.80 | 0.88 |
| 5 | 0.90 | 0.88 | 1.14 | 1.12 | 1.12 | 5.58 |
| 6 | 0.30 | 0.29 | 0.33 | 1.18 | 1.20 | 1.45 |
| 7 | 0.73 | 0.71 | 0.99 | 1.00 | 0.90 | 4.34 |
| 8 | 0.23 | 0.22 | 0.32 | 1.39 | 1.39 | 1.04 |
| 9 | 0.73 | 0.72 | 0.98 | 1.12 | 1.18 | 5.58 |
| 10 | 0.25 | 0.25 | 0.32 | 1.18 | 1.20 | 1.45 |

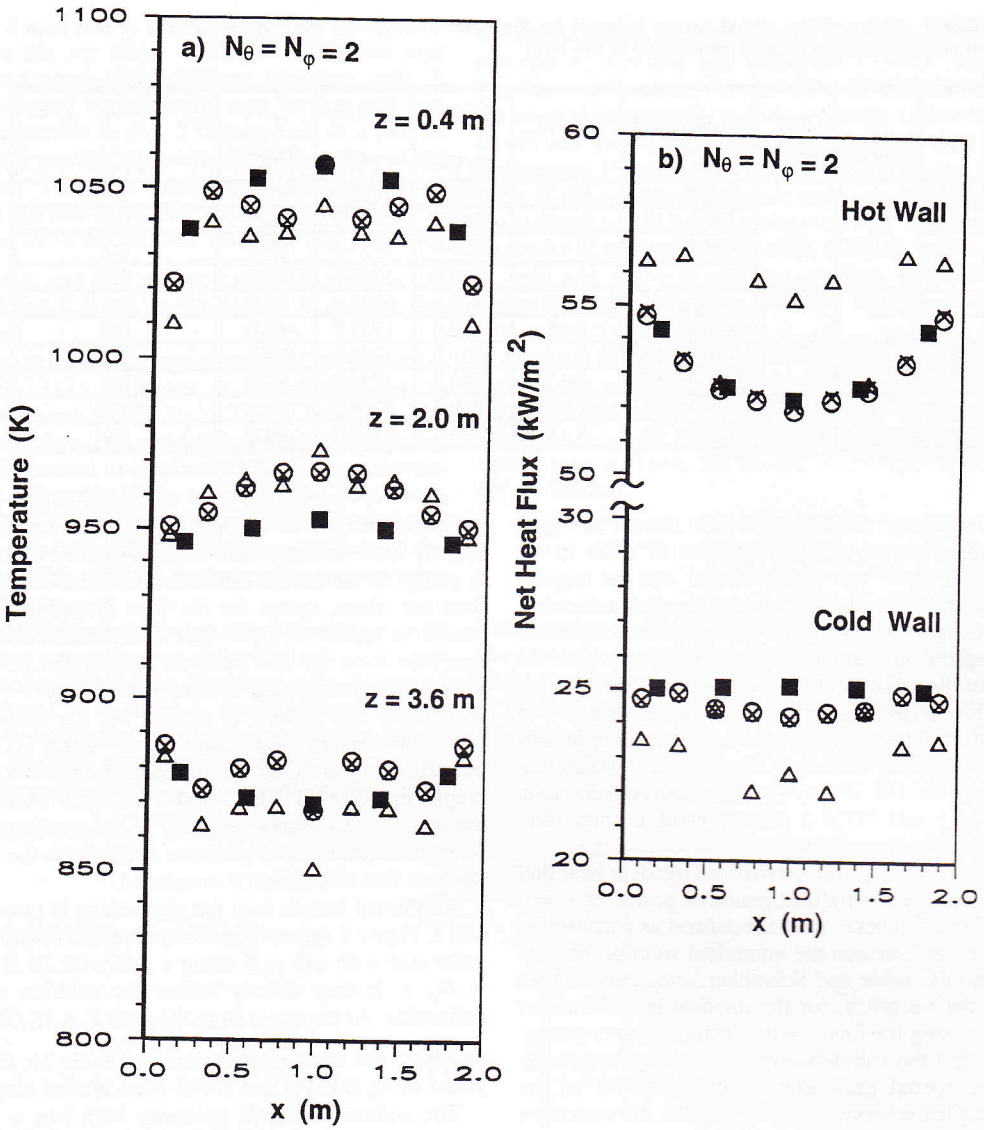


**Fig. 7** Predictions for test case 3 using $N_\theta = N_\varphi = 2$ (■—zonal method; O-DTM-0; X-DTM-1; △-DTM-2): (*a*) temperature (K) profiles; (*b*) net heat fluxes (kWm$^{-2}$).

of the three methods are similar and close to the solution of Crosbie and Schrenker, as shown in Fig. 5. However, even this discretization is unable to reproduce the incident heat flux on the bottom wall, not shown here. This is explained by the shape of the enclosure and the boundary conditions. Only the top wall is hot, and the gas temperature is only significant close to this wall, up to $y/b \approx 0.2$ (Fig. 5*a*). Therefore, radiosity rays fired from the bottom wall must reach the top region of the enclosure to contribute to the incident heat flux at the bottom wall. Since $b/a$ is large, only a few radiosity rays actually reach the top region, especially if they are fired from $x$ close to zero. This is the so-called ray effect (Lathrop, 1968; Chai et al., 1993) which is also responsible for the nonmonotonic convergence and the lack of accuracy at coarse resolution. It explains the need to use a very fine angular discretization ($N_\theta = N_\varphi = 20$) to satisfactorily predict the incident heat flux on the bottom wall (Fig. 5*d*).

**Test Case 2—Two-Dimensional Transient Combined Conduction-Radiation Problem.** A two-dimensional rectangular black enclosure with $a/b = 5$ is considered again in this test case. A transient coupled conductive and radiative heat transfer problem is analyzed to show the accumulation of errors in the energy balance along the time. The mathematical formulation of the problem for an anisotropic scattering medium in dimensionless form is given by the following equations:

$$\frac{\partial \theta}{\partial t^*} = \frac{\partial^2 \theta}{\partial \tau_x^2} + \frac{\partial^2 \theta}{\partial \tau_y^2} - \frac{1}{N} \nabla \cdot Q$$

$$-\beta a < \tau_x < \beta a, \quad 0 < \tau_y < \beta b, \quad t^* > 0 \tag{23}$$

where

$$\nabla \cdot Q = (1 - \omega)\left(4\theta^4 - \int_{4\pi} \psi d\Omega\right) \tag{24}$$

and

$$\frac{d\psi}{d\tau_s} = -\psi + \frac{(1 - \omega)}{\pi} \theta^4 + \frac{\omega}{4\pi} \int_{4\pi} \psi d\Omega. \tag{25}$$

The dimensionless quantities are defined as

$$\tau_x = \beta x, \quad \tau_y = \beta y, \quad \tau_s = \beta s, \quad t^* = \alpha \beta^2 t,$$

$$\theta = T/T_o, \quad N = k\beta T_o/(\sigma T_o^4),$$

$$Q = q/(\sigma T_o^4), \quad \psi = I/(\sigma T_o^4). \tag{26}$$

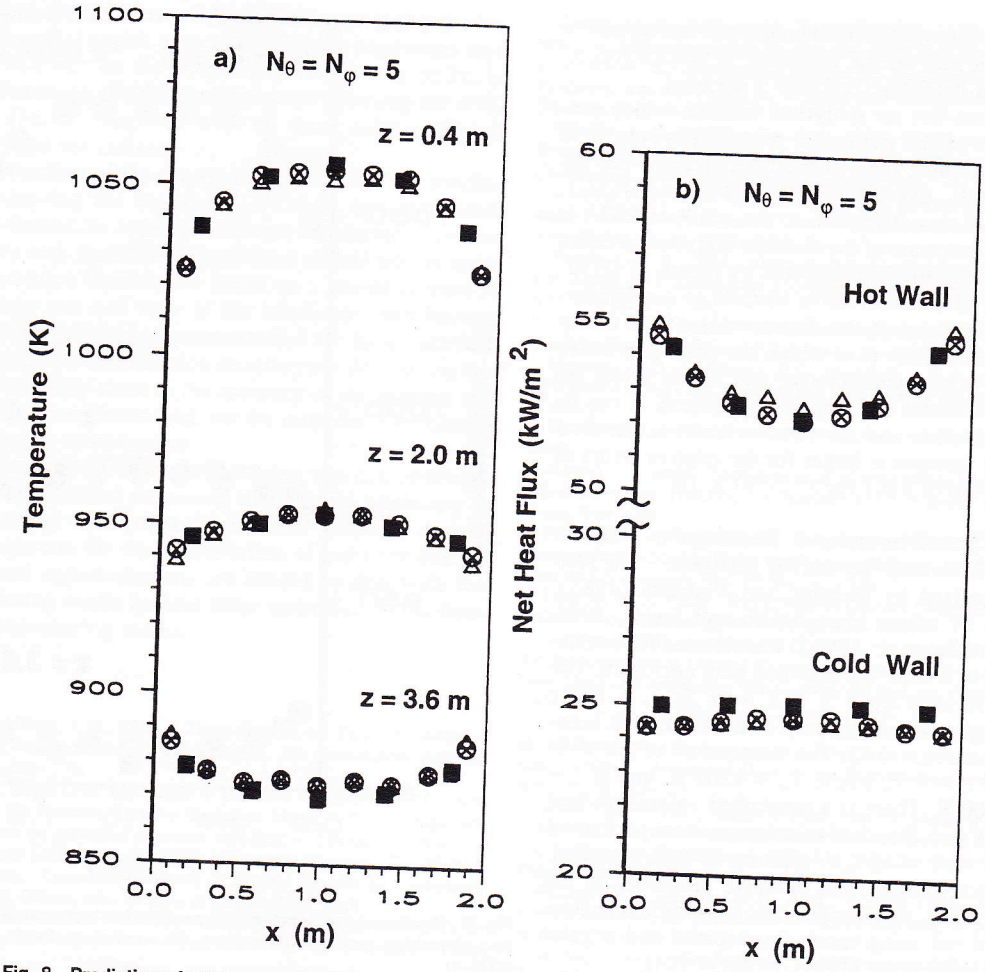


Fig. 8 Predictions for test case 3 using $N_\theta = N_\varphi = 5$ (■—zonal method; O-DTM-0; X-DTM-1; Δ-DTM-2): (*a*) temperature (K) profiles; (*b*) net heat fluxes (kWm$^{-2}$).

At $t^* = 0$, the temperature of the medium and top wall is $T_o$, and the temperature of the remaining walls is zero. The temperature of the boundaries is kept constant along the time. Therefore, the initial and boundary conditions of Eq. (23) become

$$\theta(\pm\beta a, \tau_y, t^*) = \theta(\tau_x, \beta b, t^*) = 0,$$

$$\theta(\tau_x, 0, t^*) = 1, \quad \text{for} \quad t^* > 0$$

$$\theta(\tau_x, \tau_y, 0) = 1,$$

$$\text{for} \quad -\beta a < \tau_x < \beta a, \quad 0 < \tau_y < \beta b. \quad (27)$$

Notice that if the conduction to radiation parameter, $N$, were equal to zero, the present problem would be simplified, becoming precisely the purely radiative heat transfer problem studied in test case 1.

The energy conservation Eq. (23) was solved using a finite volume/finite difference method, and the fully implicit method was employed for time discretization (Gosman et al., 1985). Calculations were performed for $\omega = 0$, $\beta = \kappa = 1$, $\sigma T_o^4 = 1$, and $N = 1$. A discretization with $80 \times 40$ control volumes, $N_\theta = N_\varphi = 10$ and $\Delta t^* = 10^{-4}$ was selected. The accuracy of the time discretization was checked by repeating the calculations using a time step equal to $0.5 \times 10^{-4}$. It was found that the numerical solution is independent of $\Delta t^*$ for the two reported values.

Figure 6*a* shows the symmetric of the unsteady, conductive, and radiative terms of Eq. (23) integrated over the whole domain from 0 to $t^*$, with $t^* \leq 1.5 \times 10^{-2}$:

$$E_1 = \int_{-\beta a}^{\beta a}\int_0^{\beta b}\int_0^{t^*} \frac{\partial\theta}{\partial t}\, dt d\tau_y d\tau_x \quad (28a)$$

$$E_2 = \int_{-\beta a}^{\beta a}\int_0^{\beta b}\int_0^{t^*} \left(\frac{\partial^2\theta}{\partial\tau_x^2} + \frac{\partial^2\theta}{\partial\tau_y^2}\right) dt d\tau_y d\tau_x \quad (28b)$$

$$E_3 = \int_{-\beta a}^{\beta a}\int_0^{\beta b}\int_0^{t^*} \left(-\frac{\nabla\cdot Q}{N}\right) dt d\tau_y d\tau_x. \quad (28c)$$

The temporal evolution of the dimensionless temperature at the center of the enclosure ($\tau_x = 0$, $\tau_y = \beta b/2$) is also plotted. These results were computed using DTM-1 to solve the RTE. Since the temperature of the boundaries is fixed, the medium receives energy from the top wall and looses energy to the remaining walls by conduction and radiation. Globally, energy is released from the medium to the surroundings by radiation and conduction, up to $t^* \approx 50 \times 10^{-4}$, while the temperature of the medium decreases. For larger values of $t^*$, the medium still looses energy by conduction but its temperature is already small enough such that $\nabla \cdot Q$ becomes negative. The conductive and the radiative terms of Eq. (23) tend to compensate each other such that the temperature of the medium and the total energy release level off as steady state is approached for large values of $t^*$.

The numerical method used to solve Eq. (23) is conservative and, therefore, the numerical solution satisfies the global energy balance $E_1 = E_2 + E_3$, regardless of the method used to solve the RTE. However, if DTM-0 is used, the dimensionless form of Eq. (13) is not satisfied. Hence, the value of $\nabla \cdot Q$ fed into Eq.

(23), integrated over the whole domain, does not correspond to the net radiative heat rate on the boundary of the enclosure. This does not happen if DTM-1 or DTM-2 are used.

The present problem has no analytical solution which prevents the calculation of the numerical errors. However, it is easy to compute the absolute value of the difference between the radiative energy term $E_3$, calculated using DTM-0 and DTM-1, as well as the ratio of this difference to the result of DTM-1. These quantities are a measure of the absolute and relative errors of the radiative energy term E3 calculated by means of DTM-0, taking the results of a conservative method as a reference. They quantify the imbalance in the dimensionless form of Eq. (13) and represent the extent over which the nonconservative formulation departs from a conservative one. These errors are shown in Fig. 6*b* for coarse and fine discretizations. It can be seen that both the absolute and the relative errors accumulate along the time. This increase is larger for the relative errors as a result of the decrease of $|E_3|$ for $t^* > 50 \times 10^{-4}$.

**Test Case 3—Three-Dimensional Rectangular Furnace with an Emitting-Absorbing-Scattering Medium.** The rectangular furnace idealized by Mengüç and Viskanta (1985), and also examined by others (Jamaluddin and Smith, 1988; Truelove, 1988; Carvalho et al., 1993), was selected for evaluation of the methods in a three-dimensional gray enclosure. The dimensions of the furnace are $2 \times 2 \times 4$ m$^3$ in $x$, $y$, and $z$ directions, respectively. The emissivity of the walls is 0.7, except at $z = 0$ m, where $\epsilon_w = 0.85$. The temperature of the walls is 900 K, except at $z = 0$ m, where $T_w = 1200$ K, and at $z = 4$ m, where $T_w = 400$ K. There is a prescribed volumetric heat source equal to 5 kW/m$^3$. Standard calculations were performed using a grid with $9 \times 9 \times 15$ CV, uniform in each direction. Several angular discretizations and radiative properties of the medium were considered, as described below. Additional calculations were carried out using much finer spatial and angular discretizations ($27 \times 27 \times 45$ CV, $N_\theta = N_\varphi = 10$).

The computed heat rate received and leaving the boundary of the enclosure, the radiative heat source, and the imbalance of the energy equation are listed in Table 2 for the different studied cases. The imbalance is about 0.2 percent for $N_\theta = N_\varphi = 2$, and 0.05 percent for $N_\theta = N_\varphi = 5$, regardless of the absorption and scattering coefficients. If the proposed conservative formulations are used the numerical solution satisfies the energy equation.

The mean relative errors of temperature and net heat fluxes, taking the zonal method solution reported by Truelove (1988) as a reference, are given in Table 3. DTM-2 generally yields larger errors than the others. Since the predictions of DTM-2 were also worse than the others in test case 1 and, in addition, it cannot be always applied, DTM-2 is not recommended for practical applications. The accuracy of DTM-0 and DTM-1 is similar, with slightly lower errors for the temperature if DTM-1 is used.

The predicted gas temperature distribution along the centerline of three different planes and the net heat flux along the centerline of the hot ($z = 0$ m) and cold ($z = 4$ m) walls are displayed in Fig. 7 ($N_\theta = N_\varphi = 2$) and 8 ($N_\theta = N_\varphi = 5$), for $\kappa = 0.5$ m$^{-1}$ and $\sigma_s = 0$ m$^{-1}$. The zonal method solution (Truelove, 1988) is also shown for comparison purposes. As in the previous test cases, the solution computed using DTM-1 is very close to that of DTM-0. The DTM-2 yields rather poor predictions of the net heat fluxes for $N_\theta = N_\varphi = 2$ and exhibits larger oscillations than both DTM-1 and DTM-0. A possible explanation for this behavior is that the ray effects are enhanced by the local correction of the radiation intensity leaving a boundary, yielding larger oscillations and worse predictions.

The predicted temperatures exhibit unrealistic oscillations at $z = 0.4$ m and $z = 3.6$ m for the coarser angular discretization. These wiggles are attributed to the ray effects. Nevertheless,

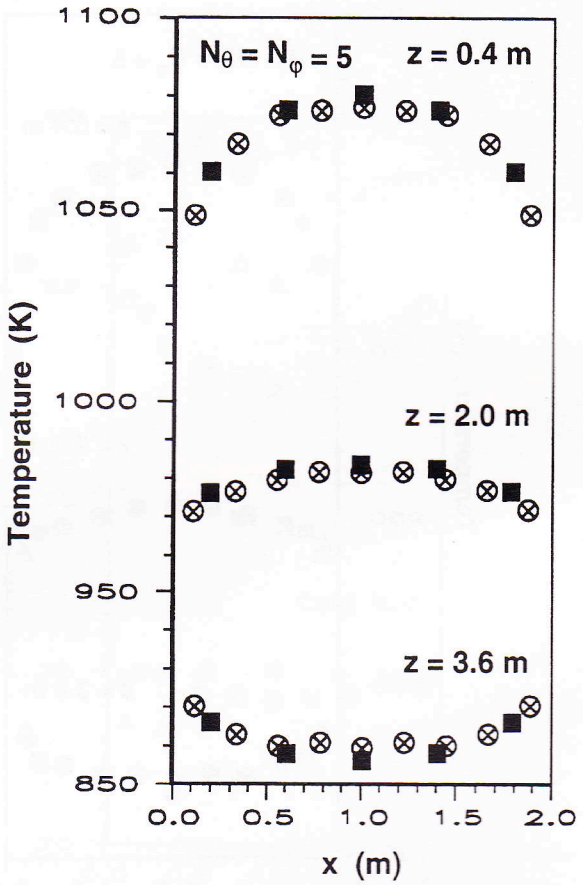


**Fig. 9 Predicted temperature (K) profiles for test case 3 with an emitting-absorbing-scattering medium (■—zonal method; O-DTM-0; X-DTM-1)**

the DTM predictions are within 20 K of the zonal method solution. Small oscillations are also observed for the net heat flux at the cold wall. If a finer angular discretization is used, the results become closer to the zonal method solution, as shown in Fig. 8. Although not shown here, similar results were obtained for nonscattering media with $\kappa = 0.25$ m$^{-1}$ and $\kappa = 1$ m$^{-1}$.

Finally, an emitting-absorbing-scattering medium with $\omega = 0.7$ and $\beta = 0.5$ m$^{-1}$ was considered, using $N_\theta = N_\varphi = 5$. The net heat fluxes are equal to those calculated for a nonscattering medium with $\kappa = 0.5$ m$^{-1}$. In fact, the radiative heat flux distribution is independent of $\omega$ for isotropic scattering with specified heat generation in the medium (Truelove, 1988). However, the emissive power of the medium increases, as shown in Fig. 9. The results obtained using DTM-0 and DTM-1 closely follow the zonal method solution. The accuracy of the results, taking the zonal method solution as the reference, is comparable to that observed for the nonscattering medium.

## Conclusions

The original formulation of the DTM was examined and new conservative formulations applicable to enclosures with diffusely emitting-reflecting boundaries were proposed and evaluated. A simple treatment for isotropic scattering media was described and validated. From the analysis carried out the following conclusions may be drawn:

1 The original formulation of the DTM is not conservative. Imbalance of the energy equation applied to an enclosure may be large if coarse spatial and angular discretizations are used. The imbalance decreases with spatial and angular refinement, but not monotonically.

2 The original formulation of the DTM is not conservative because the solid angles associated with the irradiation rays leaving a cell face on the boundary do not add up to $2\pi$, in general. Therefore, if the radiation intensity leaving the wall, taken as $J/\pi$, is integrated over all those solid angles, it does not yield the radiosity $J$.
3 A local correction of the energy per unit time of the irradiation rays leaving the boundary (DTM-2) was evaluated. However, the results obtained were not satisfactory in terms of accuracy and, therefore, this method should not be used.
4 The conservative formulation based on a global correction of the energy per unit time of the irradiation rays leaving the boundary (DTM-1) is recommended for future applications of the DTM. The solution accuracy obtained using this formulation is very close to the accuracy of the original one for all the test cases examined, but the proposed formulation satisfies energy conservation.
5 A simple treatment of isotropic scattering was demonstrated. The proposed method calculates the integral appearing in the in-scattering term using the incident radiation derived from the equation for the conservation of radiative energy. No additional approximations are needed to deal with isotropic scattering media besides those embodied in the treatment of nonscattering media.

## References


Boyd, R. K., and Kent, J. H., 1986, "Three-dimensional Furnace Computer Modelling," *21st Symposium (Int.) on Combustion,* The Combustion Institute, Pittsburgh, PA, pp. 265–274.

Bressloff, N. W., Moss, J. B., and Rubini, P. A., 1995, "Application of a New Weighting Set for the Discrete Transfer Radiation Model," *Proceedings, 3rd European Conference on Industrial Furnaces and Boilers,* Lisbon, Portugal.

Carlson, B. G., and Lathrop, K. D., 1968, "Transport Theory—The Method of Discrete Ordinates," *Computing Methods in Reactor Physics,* H. Greenspan, C. N. Kelber, and D. Okrent, eds., Gordon & Breach, New York.

Carvalho, M. G., and Coelho, P. J., 1989, "Heat Transfer in Gas Turbine Combustors," *Journal of Thermophysics and Heat Transfer,* Vol. 3, No. 2, pp. 123–131.

Carvalho, M. G., Farias, T., and Fontes, P., 1993, "Multidimensional Modeling of Radiative Heat Transfer in Scattering Media," ASME JOURNAL OF HEAT TRANSFER, Vol. 115, pp. 486–489.

Chai, J. C., Lee, H. S., and Patankar, S., 1993, "Ray Effect and False Scattering in the Discrete Ordinates Method," *Numerical Heat Transfer,* Part B, Vol. 24, pp. 373–389.

Chai, J. C., Lee, H. S., and Patankar, S. V., 1994, "Finite Volume Method for Radiation Heat Transfer," *Journal of Thermophysics and Heat Transfer,* Vol. 8, pp. 419–425.

Coelho, M. G., Gonçalves, J. M., and Carvalho, M. G., 1995, "A Comparative Study of Radiation Models for Coupled Fluid Flow/Heat Transfer Problems," *Proceedings, 9th International Conference for Numerical Methods in Thermal Problems,* Vol. IX, Part 1, R. W. Lewis and P. Dubertaki, eds., Pineridge Press, Swansea, pp. 378–389.

Crosbie, A. L., and Schrenker, R. G., 1984, "Radiative Heat Transfer in a Two-Dimensional Rectangular Medium Exposed to Diffuse Radiation," *Journal of Quantitative Spectroscopy and Radiative Transfer,* Vol. 31, No. 4, pp. 339–372.

Cumber, P. S., 1995, "Improvements to the Discrete Transfer Method of Calculating Radiative Heat Transfer," *International Journal of Heat and Mass Transfer,* Vol. 38, No. 12, pp. 2251–2258.

Fiveland, W. A., 1984, "Discrete-Ordinates Solutions of the Radiative Transport Equation for Rectangular Enclosures," ASME JOURNAL OF HEAT TRANSFER, Vol. 106, pp. 699–706.

Gosman, A. D., Launder, B. E., and Reece, G. J., 1985, *Computer-Aided Engineering, Heat Transfer and Fluid Flow,* John Wiley & Sons, New York.

Gosman, A. D., Lockwood, F. C., Megahed, I. E. A., and Shah, N. G., 1982, "Prediction of the Flow, Reaction and Heat Transfer in a Glass Furnace," *Journal of Energy,* Vol. 6, No. 6, pp. 353–360.

Hottel, H. C., and Sarofim, A. F., 1967, *Radiative Transfer,* McGraw-Hill, New York.

Howell, J. R., 1968, "Application of Monte Carlo to Heat Transfer Problems," *Advances in Heat Transfer,* J. P. Hartnett and T. F. Irvine, eds., Vol. 5, Academic Press, New York.

Jamaluddin, A. S., and Smith, P. J., 1988, "Predicting Radiative Transfer in Rectangular Enclosures Using the Discrete Ordinates Method," *Combustion Science and Technology,* Vol. 59, pp. 321–340.

Lathrop, K. D., 1968, "Ray Effects in Discrete Ordinates Equations," *Nuclear Science and Engineering,* Vol. 32, pp. 357–369.

Lockwood, F. C., and Shah, N. G., 1981, "A New Radiation Solution Method for Incorporation in General Combustion Prediction Procedures," *18th Symposium (Int.) on Combustion,* The Combustion Institute, Pittsburgh, PA, pp. 1405–1414.

Mengüç, M. P., and Viskanta, R., 1985, "Radiative Transfer in Three-Dimensional Rectangular Enclosures Containing Inhomogeneous Anisotropically Scattering Media," *Journal of Quantitative Sprectroscopy and Radiative Transfer,* Vol. 33, pp. 533–549.

Modest, M. F., 1993, *Radiative Heat Transfer,* McGraw-Hill, New York.

Murthy, J. Y., and Choudhury, D., 1992, "Computation of Participating Radiation in Complex Geometries," HTD-Vol. 203, *Developments in Radiative Heat Transfer,* ASME, New York, pp. 153–160.

Raithby, G. D., and Chui, E. H., 1990, "A Finite Volume Method for Predicting Radiant Heat Transfer in Enclosures with Participating Media," ASME JOURNAL OF HEAT TRANSFER, Vol. 112, pp. 415–423.

Selçuk, N., 1983, "Evaluation of Multi-Dimensional Flux Models for Radiative Transfer in Combustion Chambers: A Review," AGARD CP-353, Paper No. 28.

Shah, N. G., 1979, "New Method of Computation of Radiation Heat Transfer in Combustion Chambers," Ph. D. Thesis, Imperial College of Science and Technology, London.

Truelove, J. S., 1988, "Three-dimensional Radiation in Absorbing-Emitting-Scattering Media using the Discrete-Ordinates Approximation," *Journal of Quantitative Spectroscopy and Radiative Transfer,* Vol. 39, No. 1, pp. 27–31.

Viskanta, R., and Mengüç, M. P., 1987, "Radiation Heat Transfer in Combustion Systems," *Progress in Energy and Combustion Science,* Vol. 13, pp. 97–160.